Faculty V - Math and Natural Sciences

Lab Project II

Homogeneous Heating Techniques for Detecting Laminar-Turbulent Transitions using Infrared Thermography

Fynn Völker 5941217 / Tim Gerlach 5911797
Supervisor: Dr. rer. nat. Tom Wester
Date: May 12, 2024

Contents

1 Introduction

The understanding of laminar flow, turbulent flow and especially the transition zone between the two flow types has been a great challenge for ongoing research. Since their properties are of high interest for several wind energy research institutes, the study of this topic remains the focus of many minds. Due to the fact, that these flow transition areas can be observed using infrared thermography (if a temperature difference between the ambient temperature and temperature of a wind turbine blade exists), methods for the creation of a homogeneous temperature gradient will be the core of this project. Furthermore these methods will be tested inside a wind tunnel and are discussed with regard to their applicability.

2 Theoretical Background

Thermal radiation emitted by every object with a temperature greater than absolute zero (T>0K), which is commonly described by the black body radiation law, is a well known phenomenon in physics. Using a high end infrared camera, such as the one used in Chapter 3, the emitted infra red spectrum (wavelengths in the range of $\lambda \approx 1\mu m$ to $\lambda \approx 1mm$) may be recorded and analyzed to get the temperature of the emitting body, even at low temperatures. This process is called infrared thermography and a resolution of about $\Delta T \leq 15mK$ can be achieved[3]. One of the possible applications of this technique is to analyze the change in surface temperature in an aerodynamic system due to convection, in order to analyse influences of laminar and turbulent flow at the surface of an object such as air turbine blades. This works because in a turbulent boundary layer the transfer of heat and the momentum of the turbulent flow are related via Reynold's analogy, seen in Equation 1[1][2].

$$\frac{c_f}{2} = \frac{h_c}{c_p G} \tag{1}$$

Where h_c is the heat transfer via convection, c_p is the specific heat capacity of the fluid and G is the mass transport inside the fluid. From this it is possible to deduce that the temperature and velocity profiles must have the same shape[3]. Introducing the Stanton number St with some simplifications[1][2] as

$$St = \frac{h_c}{c_p G} \tag{2}$$

it directly follows that

$$St = \frac{c_f}{2} = \frac{h_c}{c_p G}. \tag{3}$$

Which for this purpose may be simplified to

$$St \approx c_f \approx h_c \tag{4}$$

Since c_f is higher for turbulent boundary layers, the transfer of heat has to increase as well, leading to a bigger heat dissipation at regions where the boundary layer is turbulent, which may directly be measured using infrared thermography[3]. For this to work at low wind speed systems, such as a wind tunnel, the surface has to be preheated or precooled to a temperature difference of approximately $\Delta T \approx 5\text{K}$ compared to the ambient temperature[3].

3 Experimental Procedure

In total, three different methods to increase the temperature of the wing homogeneously are tested. These methods consist of the usage of a heating paint, the utilisation of water as heating medium and hot air gun. For all methods temperature measurements are taken before the heating process, while heating, and after the wing is heated and brought into equilibrium between in- and outgoing heat transfer. For the measurements in the wind tunnel, the wing is brought in the equilibrium state at $\Delta T \approx 5\text{K}$ above the ambient temperature. If this state is reached, the wind tunnel is activated and the measurements are started, if the difference of the wind speed is below $0.5\frac{\text{m}}{\text{s}}$ to the desired wind speed ($\Delta v_{wind} \leq 0.5\frac{\text{m}}{\text{s}}$). All heating methods are tested for wind speeds of $v_{wind} = 10\frac{\text{m}}{\text{s}}$ and $v_{wind} = 15\frac{\text{m}}{\text{s}}$.
Measurements that provide the temperature of the wing are taken by the *InfraTec* ImageIR 8380 hp S, which provides 640 x 512 values at maximum (each pixel is assigned one temperature value).

3.1 Heating Paint

To enable a homogeneous heat transfer along the wing, also the paint needs to be applied homogeneously. Since different methods of applying the paint (using paint brushes) did not provide the desired results, spray painting seems the best suited method for this purpose. Before spray painting, the wing is foiled and the adhesive aluminium conductor strips are applied. Furthermore some insulating tape is applied to the cutting edge (underneath the aluminium conductor strips) and the sides of the wing to prevent a current flowing trough the wing itself. Another small piece of insulating tape is put on top of the aluminium conductor strips, in order to later connect the alligator clips of the current source. To ensure a equal distribution of charge carriers, the aluminium conductor strip is folded at one end (close to the cutting edge of the wing) and put on top of the other end of the aluminium strip. This procedure should ensure a similar potential at every point of the aluminum, though this has not been verified experimentally. Before the spray painting process the wing looks as seen in Figure 1.

Figure 1: Wing before the spray painting process with applied foil, aluminium conductor strips and insulating tape.

After the spray painting process, the insulating tape on top of the aluminium conductor strips and on the sides of the wing is removed. For measurements inside the wind tunnel, the wing is turned sideways and secured onto a plate using a screw. This plate is then put on top of a cube, which has mountings for the plate and a slider, which is put underneath the cube. This slider allows horizontal adjustments inside the wind tunnel. Lastly, the wing is connected to a power supply and is now ready for the measurement process. The finished product inside the wind tunnel can be seen in Figure 2.
Heating paint (C-Therm heating paint) as well as the adhesive aluminium conductor strips have been provided by *Rebotherm*, who specialize in heating solutions such as paint or foil [4].

3.2 Water Heating

To guarantee the highest possible homogeneity in terms of temperature, a powerful pump shall be used to guide a high volume of heated water with the desired temperature through the wing. For this purpose the *EHEIM compact 5000* is used, that is able to pump water with a ratio of 0.7 $\frac{\text{l}}{\text{s}}$ to 1.39 $\frac{\text{l}}{\text{s}}$, which can be

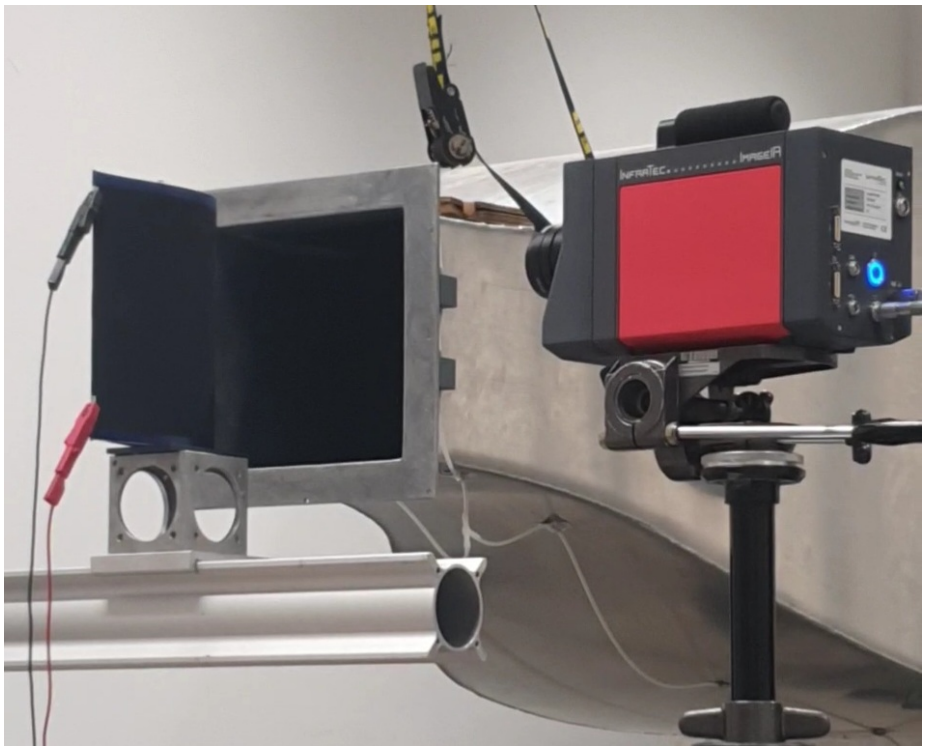

Figure 2: Finished paint heating setup inside the wind tunnel

adjusted using the turning knob on the device (though, only the lowest pump power is tested due to ensure water tightness). This pump, together with an aquarium heater, is placed into a canister. Then the pump is attached to a hose, which leads the water into the wing. Due to a rather small opening to the interior of the wing, a connection piece is installed, which brings the diameter of the hose from 24mm (outgoing from the pump) to 21mm (which barely fits into the wing). All water that is brought inside the wing, is guided back into the canister with an 21mm hose to achieve a flow cycle. For the measurements inside the wind tunnel, two cubes are mounted on the upper and lower sides of the wing to support the stability of the in- and outgoing hoses of the wing. These hoses are secured using silicone sealant, which was necessary to keep the setup watertight. The lower cube is also used to secure the wing on the slider for the measurement period. Figure 3 shows the completed setup in font of the wind tunnel. Though, it has to be mentioned, that the heating paint was still present on the wing, while the measurements are taken.

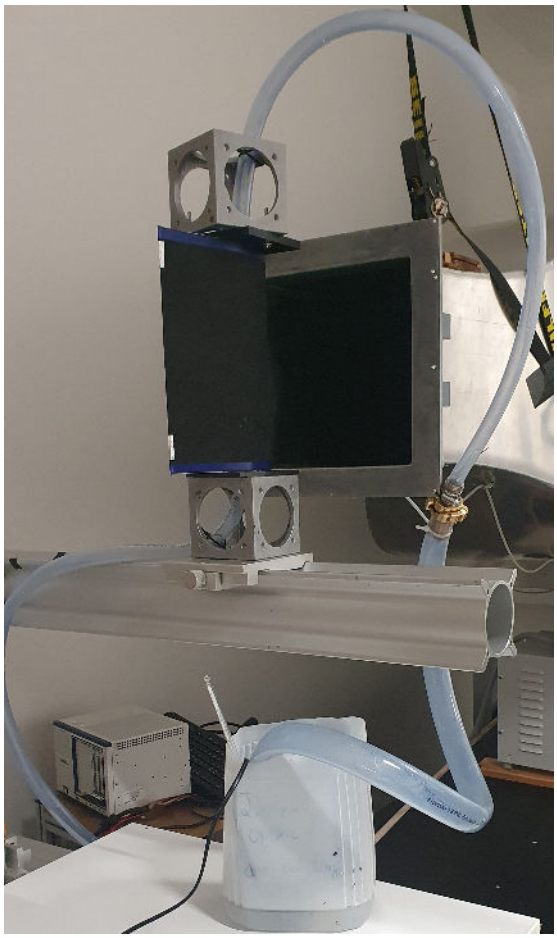

Figure 3: Setup of the water heating setup in front of the wind tunnel

3.3 Hot Air Gun Heating

To compare the newly established methods (the methods described above) with the before used method of hot air heating, the original setup is tried to be reproduced. Here a hot air gun is connected to a hose and fed into the wing (the hose is put rather far into the wing, around $\frac{2}{3}$ of the length of the wing). The lowest possible temperature setting of the gun (80°C) is used to heat the wing. Again, the wing is mounted onto the slider using the cube and the heating paint is covering the surface of the wing, as described in all other methods.

4 Measurement Results and Evaluation

In this section all measurement results are provided and evaluated. In a few cases the window of the infra red camera is adjusted, and about 10 to 20 pixels in one dimension are reduced, to only capture the region of interest. Since a matrix with $N \approx 3{\cdot}10^5$ entries is hard to read, these results are displayed in terms of pictures, that show the temperature (or temperature difference) for each pixel using a color map. Data for every method will be shown for the heated equilibrium state and after the wind tunnel is turned on. Furthermore, the heating process for all methods is measured and can be found in the Appendix (Figure 11, Figure 12, and Figure 13).

4.1 Heating Paint

To reach the state of heated equilibrium, the paint is supplied with electric power of $P \approx 10\text{W}$, with voltage in the range of $U = 5\text{V}$ to $U = 6\text{V}$ and a current of $I \approx 1.8\text{A}$. The temperature of the heated equilibrium state, together with the temperature after the wind tunnel is activated can be seen in Figure 4 (for $v_{wind} = 10\frac{\text{m}}{\text{s}}$) and Figure 5 (for $v_{wind} = 15\frac{\text{m}}{\text{s}}$). Here it can be seen, that the maximal temperature difference lies at $\Delta T_{max} \approx 0.3\text{K}$, for the heated equilibrium state, in both Figures. Furthermore it appears, that the side facing downward is slightly cooler compared to the side facing upwards. An explanation could be the mounting of the wing, since the cube that is holding the wing is attached on the lower side. This should cause the used screw to conduct heat, which should be more impactful than the heat transferred to air on the upper side. Though, this phenomenon is not investigated further in this project.
If the heated state data of Figure 4 is further analysed (with the usage of *MATLAB*), it can be shown, that the cord length at y-pixel = 400px gives a maximal temperature difference of $\Delta T_{max,cord} = 0.19\text{K}$. This maximal temperature difference would be even smaller, if the leading edge of the wing would not be considered, since the smallest temperature can be observed here. If the same procedure is repeated for the wing span at the position of x-pixel = 200px, a maximal temperature difference of $\Delta T_{max,span} = 0.29\text{K}$ is obtained.

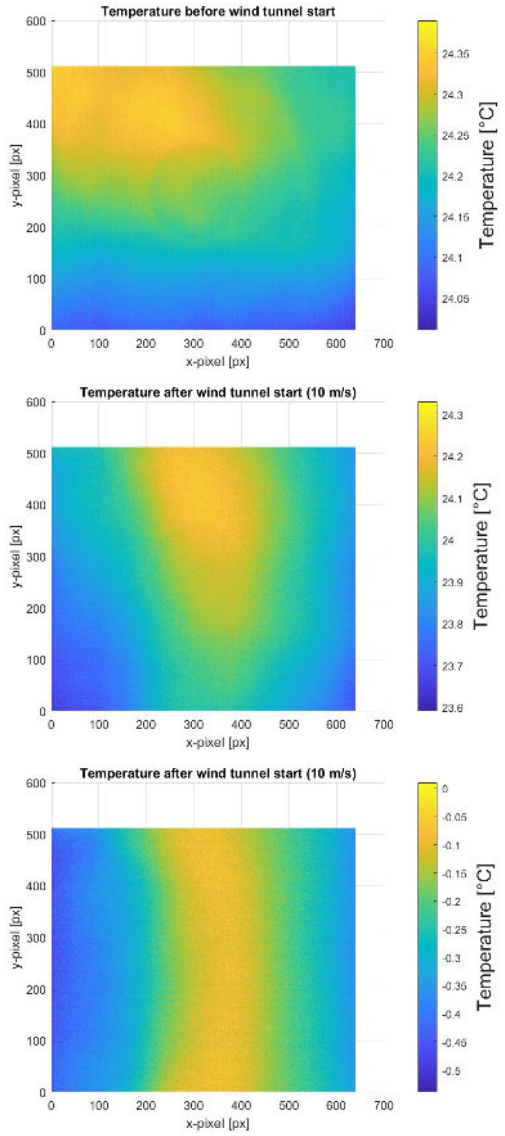

Figure 4: Temperature of the wing before a wind tunnel start (heated by the heating paint), after the wind tunnel is commuted to $v_{wind} = 10\frac{\mathrm{m}}{\mathrm{s}}$, and the temperature difference between both cases.

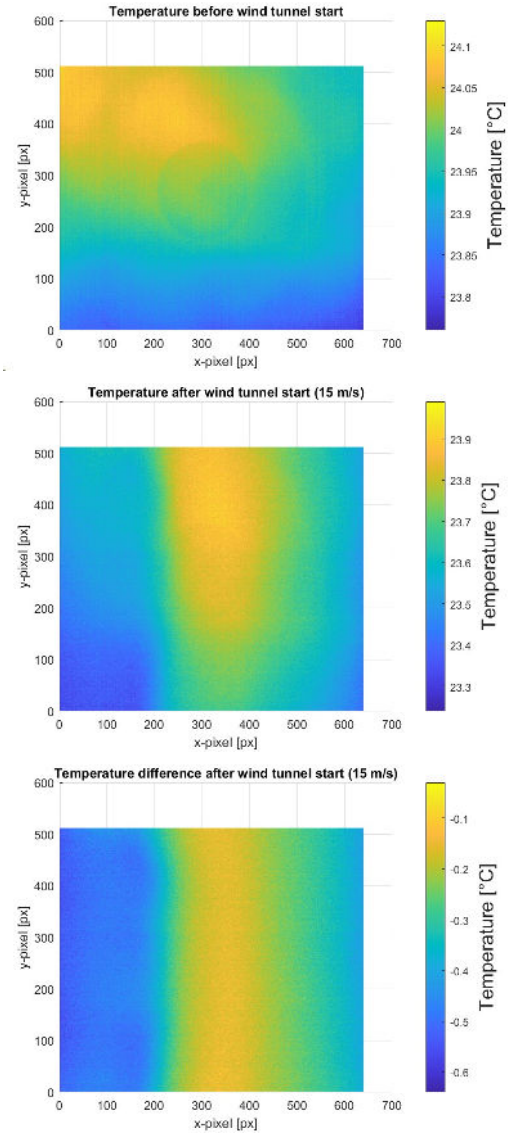

Figure 5: Temperature of the wing before a wind tunnel start, after the wind tunnel is commuted to $v_{wind} = 15\frac{\mathrm{m}}{\mathrm{s}}$, and the temperature difference between both cases. In this case, again the heating paint is used to reach the desired temperature.

4.2 Water Heating

Measurements revolving around the water heating can be seen in Figure 6, Figure 7, and Figure 8. Here, not only the heated equilibrium state and the temper-

ature change due to wind speeds of $v_{wind} = 10\frac{\mathrm{m}}{\mathrm{s}}$ (Figure 6) and $v_{wind} = 15\frac{\mathrm{m}}{\mathrm{s}}$ (Figure 7) are investigated, but a further measurement is conducted with an higher temperature gradient of $\Delta T \approx 10\mathrm{K}$, compared to the ambient temperature (Figure 8). For all measurements, the pump is kept running while measuring, since this procedure demonstrated a more homogeneous heating of the wing (see Appendix, Figure 14). From the the above mentioned Figures, it can be observed, that the maximal temperature difference in the heated equilibrium state is around $\Delta T_{max} \approx 0.3\mathrm{K}$. Here it can be seen, that the temperature for x-pixel $\in$ [100px, 300px] only differs around $\Delta T \approx 0.1\mathrm{K}$ for all y-pixel.
If the homogeneity of the heated state of Figure 6 is further analyzed, it can be shown, that a maximal temperature difference for the cord length (again at y-pixel = 400px) can be calculated as $\Delta T_{max,cord} = 0.27\mathrm{K}$. If the same is done for the wing span at x-pixel = 200px, a maximal temperature difference of $\Delta T_{max,span} = 0.11\mathrm{K}$ is found.

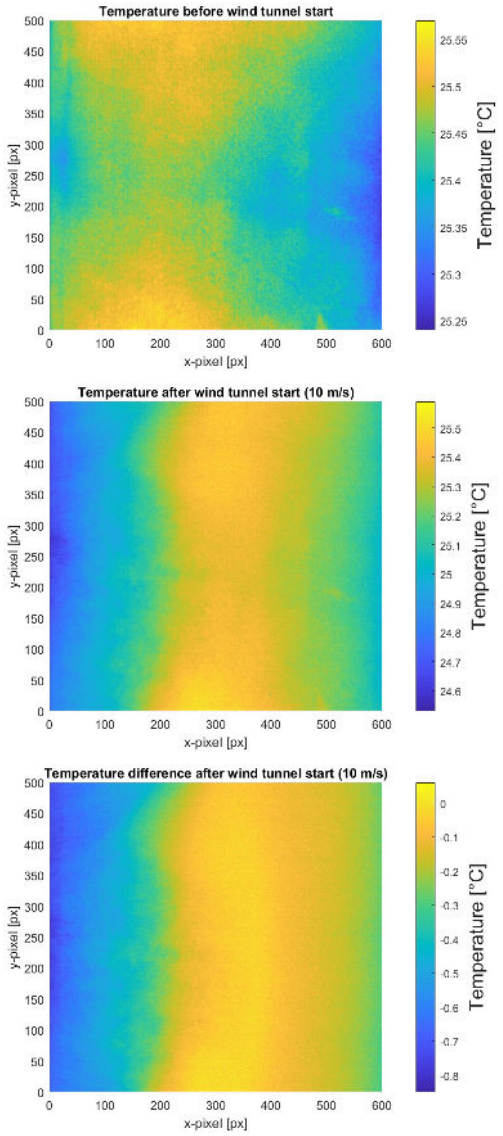

Figure 6: Temperature of the wing, that was heated by the water heating, before a wind tunnel start, after the wind tunnel is commuted to v_{wind} ($v_{wind} = 10\frac{\mathrm{m}}{\mathrm{s}}$), and the temperature difference between both cases.

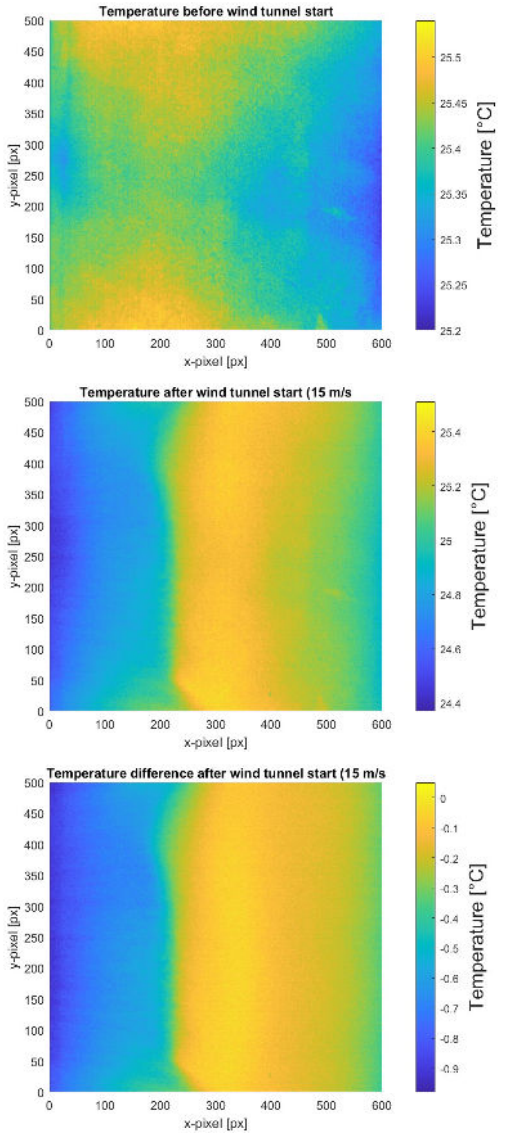

Figure 7: Temperature of the wing before a wind tunnel start ($v_{wind} = 15\frac{\mathrm{m}}{\mathrm{s}}$), after the wind tunnel is commuted to v_{wind} and the temperature difference between both cases. Water heating is used to reach the starting temperature.

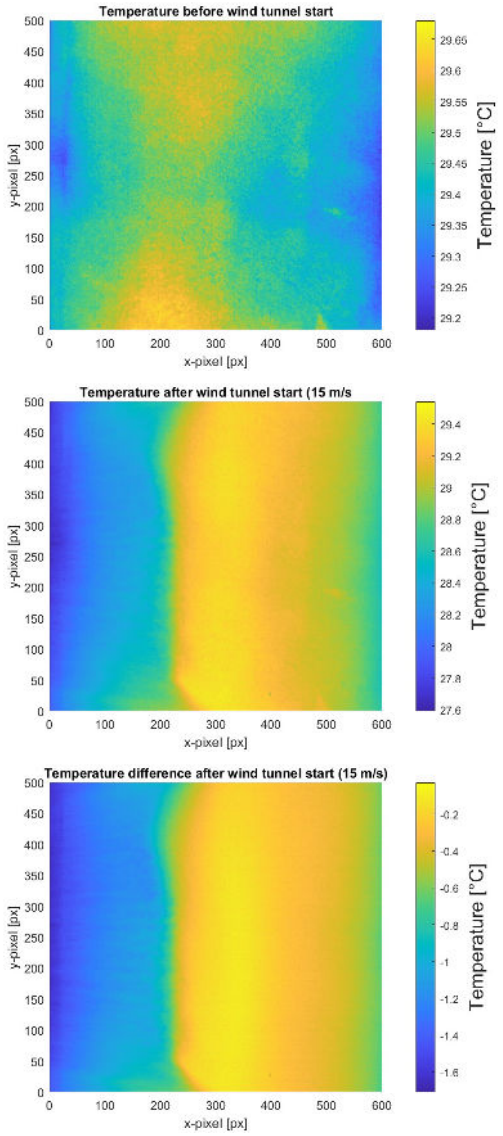

Figure 8: Temperature of the wing before a wind tunnel start ($v_{wind} = 15\frac{\mathrm{m}}{\mathrm{s}}$), after the wind tunnel is commuted to v_{wind}, and the temperature difference between both cases. Water heating is used to reach the starting temperature, which in this case is kept around 30°C instead of 25°C.

4.3 Hot Air Gun Heating

Figure 9 and Figure 10 show the temperature measurements in the wind tunnel, before and after a wind speed of $v_{wind} = 10\frac{\mathrm{m}}{\mathrm{s}}$ (Figure 9) or $v_{wind} = 15\frac{\mathrm{m}}{\mathrm{s}}$ (Figure 10) is applied. Here, the wing is heated using the heat gun. It has to be mentioned, that the wing has a highly inhomogeneous temperature profile after the heating process (see Appendix, Figure 13) and thus is cooled down for a few minutes before the measurements are conducted. This brought the maximal temperature difference to around $\Delta T_{max} \approx 0.8\mathrm{K}$. Again, as with the heating paint, the temperature in the lower part of the wing is lower compared to the upper part. This can not only be explained by the cube, that is mounted underneath the wing (which leads to heat conduction), but also by the positioning of the hose, which causes the hot air to flow against the upper side of the interior of the wing. Though, a further method, that is distributing the hot air more evenly, is not tested.
A further analysis of the heated state data of Figure 9 shows a maximal temperature difference over the cord length (y-pixel = 400px) and wing span (x-pixel = 200px) of $\Delta T_{max,cord} = 0.23\mathrm{K}$ and $\Delta T_{max,span} = 0.46\mathrm{K}$.

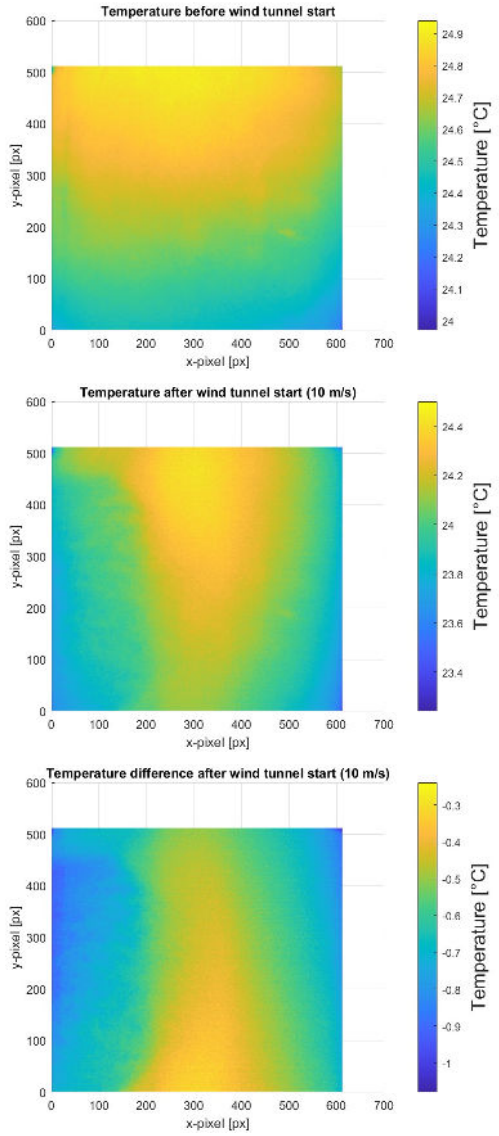

Figure 9: Temperature of the wing before a wind tunnel start, after the wind tunnel is commuted to $v_{wind} = 10\frac{\mathrm{m}}{\mathrm{s}}$, and the temperature difference between both cases. For these measurements, the heat gun is used to reach the starting temperature

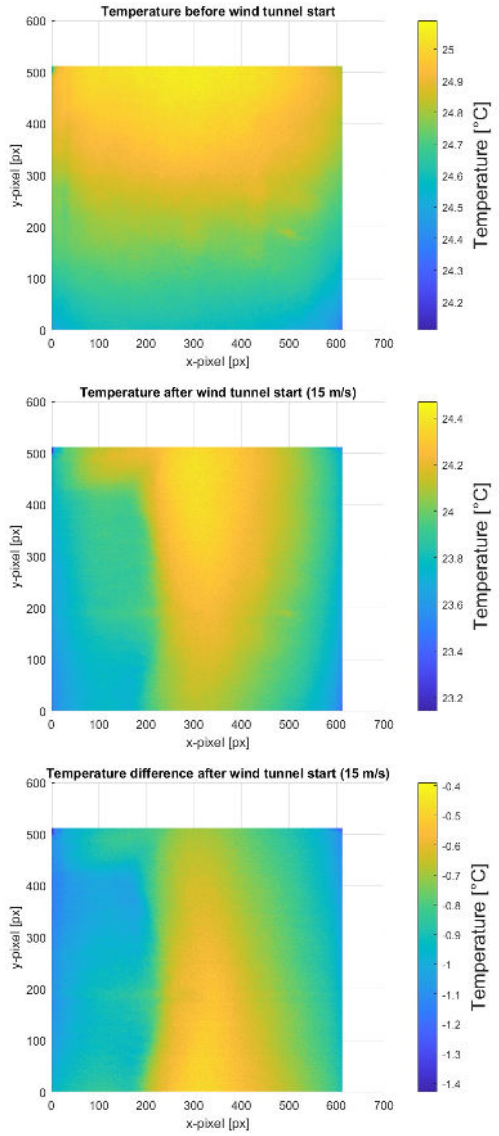

Figure 10: Temperature of the wing before a wind tunnel start, after the wind tunnel is commuted to $v_{wind} = 15\frac{\mathrm{m}}{\mathrm{s}}$, and the temperature difference between both cases. For these measurements, again the heat gun is used to reach the desired temperature

5 Conclusion

From Chapter 4, it appears that the tested heating techniques offer different advantages in terms of achieving the desired homogeneous elevation of the tem-

perature of the wing. While the heating paint performed best along the cord length (with $\Delta T_{max,cord} = 0.19\text{K}$) , the water heating method obtained the most homogeneous measurements across the wing span, with $\Delta T_{max,span} = 0.11\text{K}$. The hot air heating method did slightly outperform the water heating method in terms of homogeneity along the cord length, but came last in all other aspects. One of these aspects is the maximal temperature difference ΔT_{max} across the whole wing, which lies around $\Delta T_{max} \approx 0.8\text{K}$ for the hot air gun method (compared to $\Delta T_{max} \approx 0.3\text{K}$, which was measured for both other methods). A clear separation of laminar and turbulent flow areas due to the temperature profile could not be found, which may be caused by the rough surface of the heating paint, which was preset for all measurements. Since the homogeneous heating procedure is the main focus of this project, this has not been further investigated.

When all methods are set side by side in terms of practicality, it has to be mentioned, that the heating paint method is easiest to use, once the paint is applied according to Chapter 3.1. The water heating method takes about 20 minutes to heat up to the desired temperature of around 25°C (though, conveniently stays at that temperature after the aquarium heater is turned off). For the hot air gun, the wing needs around 10 minutes of rest time after the heating process to ensure adequate homogeneity, while the heating paint can be used within five minutes after supplying electrical power. Even though the water heating method shows great results in terms of homogeneity along the span width of the wing, its setup is not practical for general use cases, since slight adjustments of the cumbersome setup jeopardize the water tightness of the system.

Conclusively, it can be said, that the heating paint provides homogeneous heating and practicality, while both other methods only serve with one of these attributes.

6 Bibliography

References

[1] *Dawid Taler*, Numerical Modelling and Experimental Testing of Heat Exchangers, Cracow, 2019

[2] *S. P. Venkateshan*, Heat Transfer 3e, Chennai, 2021

[3] *T.T.B Wester*, Dessertation:Tailored inflow fields and the resulting aerodynamic phenomena unfolded using Particle Image Velocimetry, Oldenburg, 2022

[4] https://rebotherm.de/heizanstrich-2/, last accessed on 12.05.2024

7 Appendix

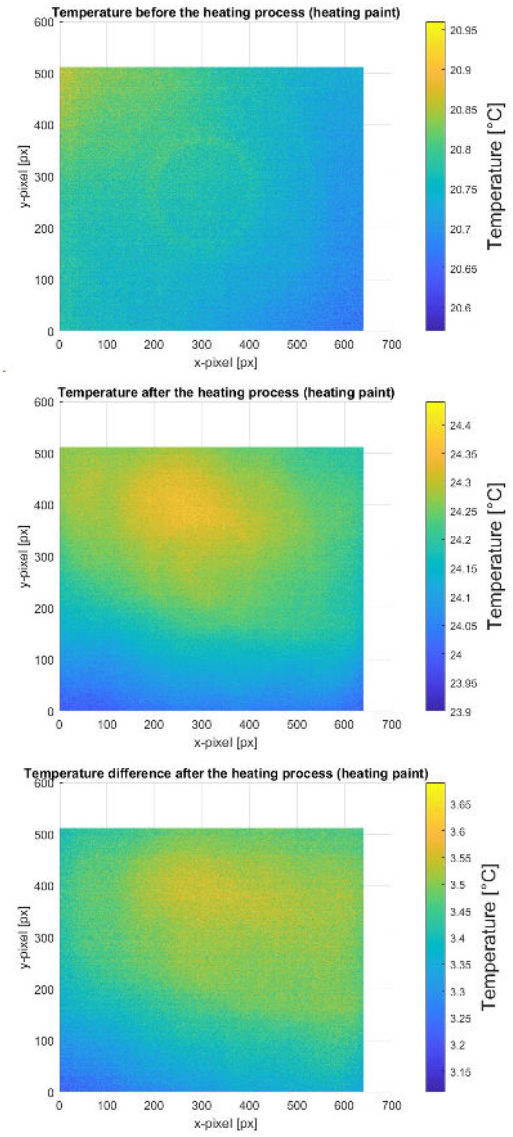

Figure 11: Temperature before the heating process with the paint, after the heating process, and the temperature difference due to the heating process.

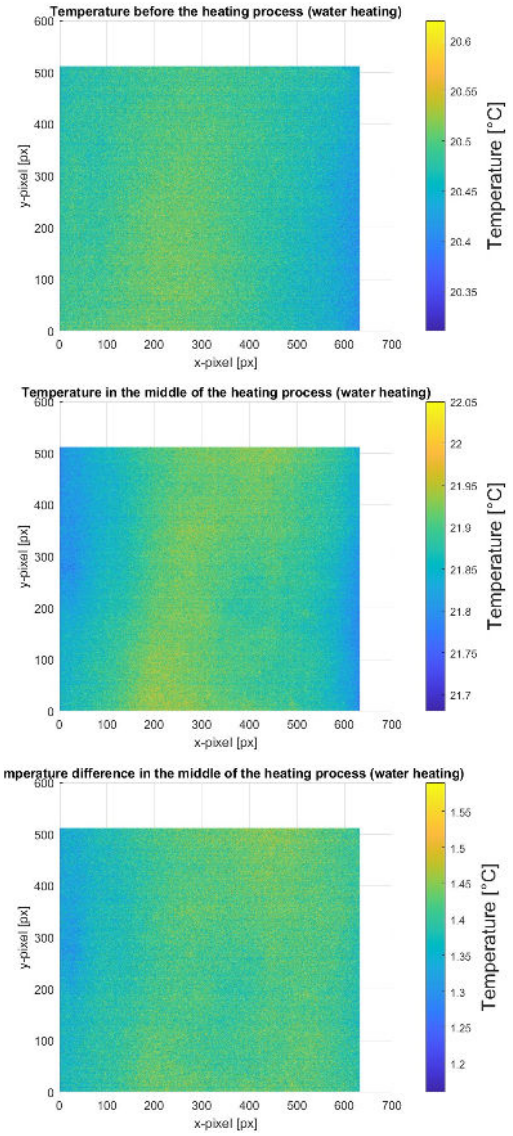

Figure 12: Temperature before the heating process with the water heating, in the middle of the heating process, and the temperature difference due to the heating process at that point.

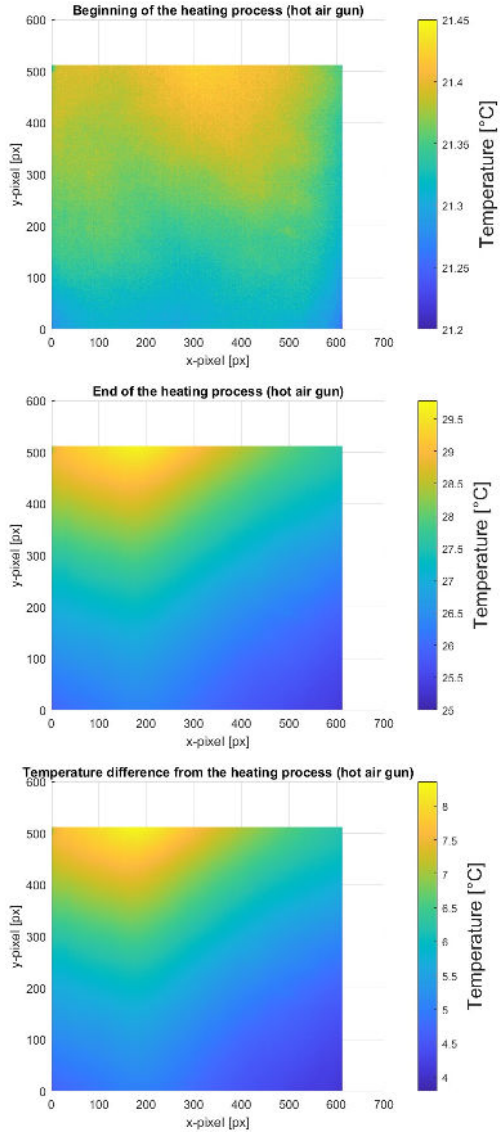

Figure 13: Temperature before the heating process with the hot air gun, after the heating process, and the temperature difference due to the heating process.

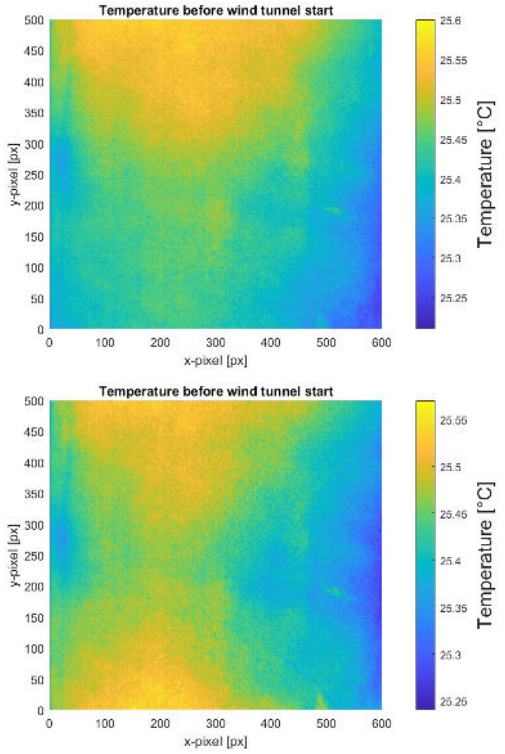

Figure 14: Temperature in heated equilibrium state when the pump was not running (upper image) and when the pump was running (lower image).